Generation of Broadband VUV Light Using Third-Order Cascaded Processes

L. Misoguti, S. Backus, C. G. Durfee,* R. Bartels, M. M. Murnane,† and H. C. Kapteyn

JILA and Department of Physics, University of Colorado at Boulder, Boulder, Colorado 80309-0440

(Received 2 August 2000; revised manuscript received 1 February 2001; published 14 June 2001)

We report the first demonstration of broadband VUV light generation through cascaded nonlinear wave mixing in a gas. Using a hollow-fiber geometry to achieve broad-bandwidth phase-matching, frequency conversion of ultrashort-pulse Ti:sapphire laser pulses from the visible into the deep UV around 200 and 160 nm is achieved. A new type of quasi-phase-matching is also observed in the VUV for the first time. Conversion using cascaded processes exhibits higher efficiencies, shorter pulse durations, and broader bandwidths than other schemes for generating light in the deep UV, and will enable many applications in science and technology.

DOI: 10.1103/PhysRevLett.87.013601 PACS numbers: 42.50.Gy, 42.65.Ky, 42.65.Wi, 42.81.Qb

Nonlinear optical techniques have been used extensively to extend the wavelength range of coherent light sources, making it possible to efficiently generate light in the visible and ultraviolet (UV) regions of the spectrum. In this Letter, we describe a new approach in nonlinear optics for the generation of ultra-short-pulse, short-wavelength light. In past work using a hollow-waveguide geometry for frequency conversion [1–3], we demonstrated that it is possible to achieve high efficiency conversion into the UV and soft-x-ray regions of the spectrum. In this Letter, we show that this high efficiency allows us to drive a cascaded nonlinear up-conversion process from the visible to the VUV region of the spectrum with macroscopic conversion efficiencies. Moreover, these cascaded processes are more efficient and generate broader bandwidths than past schemes, and are therefore ideal for ultra-short-pulse conversion into the VUV. Finally, we also observe a type of quasi-phase-matching in the deep-UV region of the spectrum for the first time. Cascaded four-wave mixing processes up-convert light in large (1.5 eV) energy steps (unlike processes such as anti-Stokes Raman), and are therefore uniquely suited for generating intense light in the range of photon energy 5–15 eV. This is a region of great interest for studies of small molecules, chemistry, material science, and lithography [4–6]. Chemical-physics studies, in particular, may benefit tremendously from the ability to excite shaped "wave packets" in deep-UV absorbing molecules, for applications in coherent control of molecular reactions [7,8].

Past work has demonstrated conversion efficiencies higher than 21% using nonlinear crystals to convert pulses to 208 nm [9]. However, present solid-state materials are transparent only at wavelengths longer than ~160–210 nm, and simple phase-matched harmonic generation is possible only to wavelengths of ~210 nm [10]. Furthermore, the group velocity walk-off between the fundamental and harmonic severely limits the bandwidth and pulse width in the UV [11]. Phase-matched VUV frequency conversion in gases has been achieved in the past by exploiting the negative dispersion which exists for light at wavelengths just shorter than a resonant absorption line [12–14]. However, this near-resonant requirement limits the phase-matching bandwidth, tunability, pulse width, and conversion efficiency. Electromagnetically induced transparency can also be used to obtain extremely efficient conversion of long-pulse ultraviolet light to shorter wavelengths — from 233 to 186 nm with near-unity efficiency [15], and into the VUV with more modest efficiencies [16]. Cascaded second-order nonlinear processes have also previously been studied as a means to obtain an enhanced effective third-order nonlinearity [17,18]. However, third-order cascaded nonlinear processes [19,20] have not been as extensively studied, with the exception of anti-Stokes Raman scattering, which can be used for generating deep-UV light with modest conversion efficiency [21]. In recent work, Crespo *et al.* [22] have successfully used the third-order cascaded process to extend frequency generation in solid state materials from 400–750 nm and pulsewidths of 40 fs. Cascaded frequency mixing in gases has also recently been discussed in a theoretical framework [23].

For our work, we used a gas-filled hollow-core fiber as a phase-matching medium [1]. In addition to significantly increasing the interaction length, thereby compensating for the low gas density, the guided-mode geometry allows phase-matched frequency conversion. For a waveguide of diameter a, the total wave vector for light at wavelength λ is given by

$$k(\lambda) \approx \frac{2\pi}{\lambda} + \frac{2\pi P \delta(\lambda)}{\lambda} - \frac{u_{nm}^2 \lambda}{4\pi a^2}, \qquad (1)$$

where P is the pressure of the gas, $\delta(\lambda)$ is related to the index of refraction of the gas by $n = 1 + P\delta(\lambda)$, and u_{nm} is a discrete constant that varies with the propagation mode in the fiber. The three terms in this expression correspond to the contribution from free space propagation, gas dispersion, and the waveguide dispersion, respectively. For a particular nonlinear mixing process, the net phase mismatch (Δk) is given by the vector sum of all waves involved, where the wave vector for each wave is given by Eq. (1). By adjusting the gas pressure, gas species, waveguide size, and spatial mode in which the light propagates, the phase mismatch can be tuned to achieve the phase-matching

condition of $\Delta k = mk_{\text{pump}} - qk_{\text{idler}} - k_{\text{signal}} = 0$, where m and q are the numbers of photons involved.

The experimental setup is shown in Fig. 1. Pulses at a repetition rate of 1 kHz, with an energy of 1 mJ, and duration 25 fs, are generated in a Ti:sapphire amplifier system [24]. A beam splitter directs 70% of the energy through a 250 μm thick beta-barium borate doubling crystal to generate the pump light at frequency 2ω (400 nm), which is then coupled into the hollow-core fiber of 125 μm inside diameter. The other 30% of the laser output is focused directly into the hollow-core fiber, to serve as the idler at frequency ω (800 nm). The hollow-core fiber is a fused silica capillary mounted in a cell that can be evacuated and filled with gas, typically Ar. The generated 4ω and 5ω light is spectrally resolved onto a phosphor-coated window, and detected using a charge-coupled device camera.

Light at 267 nm (3ω) is generated in the capillary using a difference-frequency four-wave mixing process (DFFWM) in argon: $3\omega = 2\omega + 2\omega - \omega$. This DFFWM process is very efficient, with about 30%–40% of the pump light at 2ω converted to 3ω. Careful mode matching and attention to the straightness has increased the efficiency by 50% over previous work [1]. Figure 2(a) shows the 3ω signal as a function of Ar pressure for a long (80 cm) and a short (10 cm) fiber. This process phase matches to the EH_{11} mode at pressures around 95 Torr [peak (3)]. For pulse energies of $\sim$25 μJ at 2ω and $\sim$30 μJ at ω, energies between 2.5 and 10 μJ were generated at 3ω in the lowest EH_{11} mode, depending on the fiber length. With such high conversion efficiency, the intensity of the 3ω light is comparable to that of the input light. This is key to making efficient cascaded conversion to still-shorter wavelengths possible.

The 267 nm (3ω) light from the first DFFWM process serves as the seed for a second four-wave mixing step, giving rise to light at either 4ω or 5ω. This second wave-mixing process can be optimized either in the same fiber or in a second, separately optimized, fiber. The output at 4ω (200 nm) and 5ω (160 nm) was monitored as a function of pressure, as shown in Figs. 2(b) and 2(c), for both short and long fibers. There are several processes that can result in each output; these are each distinguished experimentally by the phase-matching pressures, the output spatial modes, and the order of nonlinearity. For 4ω generation, the possible processes and their corresponding phase-matching pressures to the lowest possible spatial modes allowed are $4\omega = 2 \times 3\omega - 2\omega$ (12 Torr, EH_{11}; 172 Torr, EH_{12}), $4\omega = 2\omega + 3\omega - \omega$ (40 Torr, EH_{11}), $4\omega = 2 \times \omega + 2\omega$ (43 Torr, EH_{13}), and $4\omega = 3 \times 2\omega - 2 \times \omega$ (53 Torr, EH_{11}; 129 Torr, EH_{12}). The last process is a direct fifth-order process, not a cascaded process. While each process contributes to the output signal, macroscopic conversion efficiency is expected only for those processes that are phase matched, with the highest efficiency for conversion into the lowest-order EH_{11} mode of the fiber. Figure 2(b) shows the 4ω signal at 200 nm as a function of Ar gas pressure. For short (10 cm) fiber lengths, phase-matched peaks are observed at pressures of 58 and 135 Torr, while, for long (80 cm) fibers, peaks are observed at pressures of 33, 58, 95, and 135 Torr. To identify the dominant processes contributing to the observed 4ω signal, we also investigated 4ω generation in a two-stage fiber. The pressure in the first stage was adjusted and fixed to maximize 3ω generation, while the pressure in the second stage was varied, as shown in Fig. 3. We observe a single strong phase-matched peak for 4ω generation at pressures around 33 Torr, in the lowest-order EH_{11} mode of the fiber. The broad peaks at high pressures are due to phase matching to high-order spatial modes in the fiber.

We believe that strong cascaded DFFWM ($4\omega = 2\omega + 3\omega - \omega$) is the origin of peaks (1)–(3) in Fig. 2(b). Peak (1) at 33 Torr corresponds to phase matching of the $4\omega = 2\omega + 3\omega - \omega$ DFFWM process. Peak (3)

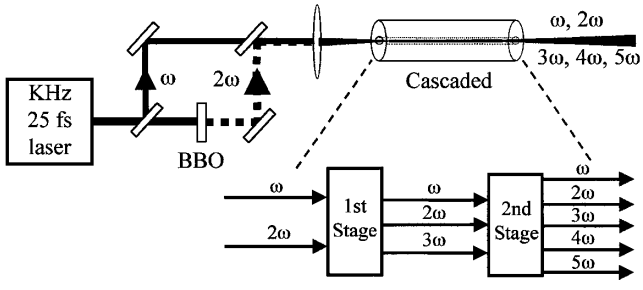

FIG. 1. Schematic diagram for cascaded guided-wave nonlinear mixing.

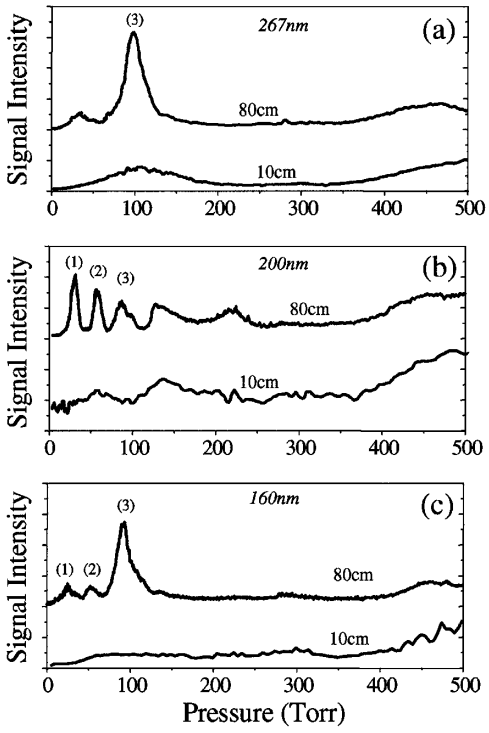

FIG. 2. Pressure tuning curves for the generation of (a) 3ω light at 267 nm, (b) 4ω light at 200 nm, and (c) 5ω light at 160 nm, within a single fiber.

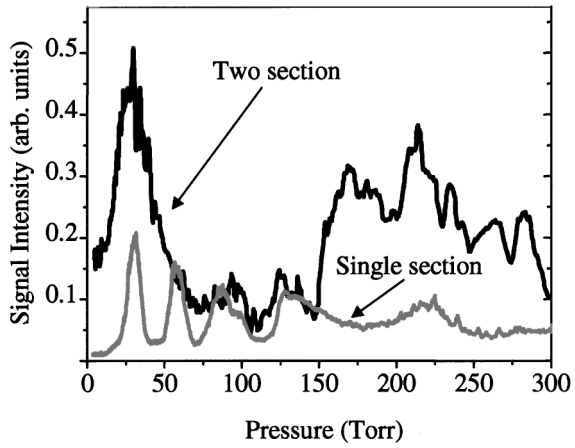

FIG. 3. Pressure tuning curves for 4ω generation in the second stage of a two-stage fiber. The pressure in the 1st stage was fixed at 100 Torr to optimize 3ω generation.

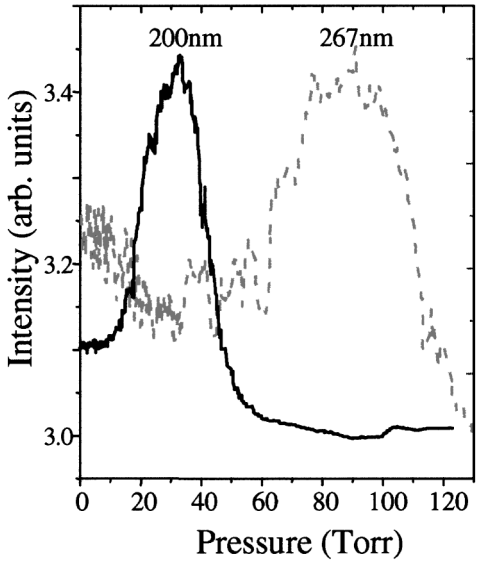

FIG. 4. Output at 3ω and 4ω as a function of pressure in the 2nd stage of a two-stage fiber. The 3ω light depletes at that pressure that optimizes 4ω generation, demonstrating a cascaded process.

corresponds to that pressure that maximizes 3ω generation—and, hence, results in a peak in 4ω generation from the same DFFWM process—despite the fact that the DFFWM process is not phase matched. Peak (2) in the long and short fiber corresponds to quasi-phase-matching of the same process within a single fiber, as will be discussed in more detail below. Several arguments support the claim of strong cascaded DFFWM as the origin of peaks (1)–(3). First, the phase-matching pressure in the long (80 cm) fiber at 33 Torr is close to the predicted value of 40 Torr (The small 7 Torr discrepancy between theory and experiment is likely due to imprecise refractive index data at short wavelengths.). Second, Fig. 3 compares 4ω generation in a long one- and two-stage fiber. In the two-stage fiber, the optimum pressure for the $4\omega = 2\omega + 3\omega - \omega$ four-wave mixing process can be adjusted independently of the 3ω generation process in the first stage. In this case, only a single pressure peak is observed for 4ω generation, at a pressure of 33 Torr, as expected for DFFWM. Third, the generated 4ω output is in the lowest-order EH_{11} mode of the fiber, as expected. Fourth, the observed dependence of the 4ω signal on 3ω power shown in Fig. 4 is consistent with this process. Fifth, evidence for depletion of the driving light at 3ω in the second stage of the two-stage fiber is shown in Fig. 4. The output 3ω light is observed to deplete at that pressure that optimizes 4ω generation.

Other possible processes that might give rise to the 4ω light can be ruled out. For example, the direct six-wave mixing process ($4\omega = 3 \times 2\omega - 2 \times \omega$) that would give rise to the 4ω signal is weak because it relies on a fifth-order nonlinearity, and it should exhibit no 3ω power dependence, in contrast to Fig. 4. For sum-frequency four-wave mixing (SFFWM), although the nonlinear susceptibility is similar to DFFWM, phase matching of this process occurs only when the signal is in a high-order mode (EH_{13} for $4\omega = 2 \times \omega + 2\omega$), which is not observed experimentally. Finally, no similar SFFWM processes are observed, even processes that should be strong such as $3\omega = \omega + \omega + \omega$, for the case of IR-only illumination.

Strong generation of light at 5ω or 160 nm was also observed, as can be seen from Fig. 2(c). Processes that generate phase-matched 5ω light are $5\omega = 2 \times 3\omega - \omega$ (18 Torr, EH_{11}), $5\omega = 4\omega + 2\omega - \omega$ (20 Torr, EH_{11}), $5\omega = 4\omega + 3\omega - 2\omega$ (6 Torr, EH_{11}), $5\omega = 2\omega + 2\omega + \omega$ (16 Torr, EH_{13}), $5\omega = 3\omega + \omega + \omega$ (6 Torr, EH_{13}), and $5\omega = 5 \times \omega$ (63 Torr, EH_{15}). As would be expected for a cascaded process, the 5ω signal intensity is observed to follow the pressure profiles of the 3ω and 4ω signal intensities, independent of the phase-matching pressure of the 5ω process. It is also generated in the lowest-order mode of the fiber. These observations restrict the possible processes giving rise to the 5ω light to a cascaded DFFWM process: either $5\omega = 2 \times 3\omega - \omega$, or $5\omega = 4\omega + 2\omega - \omega$, or $5\omega = 4\omega + 3\omega - 2\omega$.

The conversion efficiency for 4ω generation was approximately 10% of the 3ω beam, while the generated bandwidth was sufficient to support a 12 fs pulse. Cross-phase modulation by the pump can produce still larger bandwidths capable of supporting sub-4-fs pulses, when higher intensities, higher pressures, and longer fibers are employed. The conversion efficiency for 5ω generation within a single fiber was approximately 0.1% or 1% of the 3ω or 4ω light, while the generated bandwidth was sufficient to support a 6 fs pulse. For both the 4ω and 5ω signals, the stability was the same as that of the laser ($\pm 2\%$), because we saturate the output.

Simple calculations based on Eq. (1) above can predict the phase-matching pressure, power dependence, and output modes for the various processes involved in the generation of the 4ω and 5ω light, as discussed above. However, an even more convincing argument can be made based on a model that keeps track of all the optical fields involved

in the interaction, and predicts the output as a sum over all possible processes. We therefore developed a more sophisticated model of the generation and propagation of light at the first through fifth harmonic, where the five coupled nonlinear equations are solved for given pulse input, waveguide dimension, gas type, and pressure. The Fourier split-step method is used to model the propagation of the fields: Full expressions for the refractive index of the gas [25] and waveguide [26] are computed in the spectral domain, while in the time domain a fourth-order Runge-Kutta algorithm is used to solve the nonlinear coupled equations, including linear capillary losses. The code calculates frequency generation and back-conversion while accounting for phase and group velocity mismatch effects. All phase-matchable third-order frequency mixing terms are included, as well as self- and cross-phase modulation effects that tend to broaden the pulse spectra. Nonlinear coefficients are available in the literature [27].

For 4ω generation based on DFFWM ($4\omega = 3\omega + 2\omega - \omega$), the predicted phase-matched ($\Delta k_4 = 0$) pressures based on this more sophisticated model are 40 and 143 Torr for the two lowest-order modes EH_{11} and EH_{12}, respectively. This is in agreement with experimental observations and simple calculations. For cascaded process within a single fiber, the generation of light at 4ω also depends on the phase mismatch in the generation of 3ω. When $\Delta k_3 + \Delta k_4 = 0$, the field at 3ω oscillates at the same period as the 4ω phase mismatch. This corresponds to quasi-phase-matched generation of 4ω light—the 3ω pump is present predominantly when it contributes "in phase" to the 4ω field. Numerical integration confirms that the signal at 4ω will also peak at pressures of 53 and 129 Torr for the EH_{11} and EH_{12} modes, respectively, where $\Delta k_3 + \Delta k_4 = 0$, in close agreement with Fig. 2(b). In the case of the short fiber, quasi-phase-matched generation is dominant over the direct DFFWM process, since very little pump 3ω light is available. This is the first observation of such quasi-phase-matching phenomena in the deep-UV region of the spectrum. Our calculations also predict that the 5ω output depends either on the square of the 3ω field, or linearly on both the 3ω and 4ω fields, depending upon which DFFWM process is giving rise to the signal ($5\omega = 2 \times 3\omega - \omega$, or $5\omega = 4\omega + 2\omega - \omega$, or $5\omega = 4\omega + 3\omega - 2\omega$). Because the driving fields at 3ω and 4ω are being generated within the same one-stage fiber, the 5ω signal follows the 3ω and 4ω signals independent of phase-matching pressure, as observed experimentally.

An interesting question to consider is if perturbation theory is valid at the intensities of 10^{13} W cm^{-2} used in this experiment. The validity of perturbation theory affects most of all how strong the nonlinearity is, and to a lesser extent the phase-matching conditions that are dominated by the linear index of the gas and plasma. Thus, our conclusions regarding the dominance of third-order cascaded processes for efficient, broad-bandwidth, VUV generation are valid.

In conclusion, we have demonstrated, for the first time, macroscopic conversion from the visible into the deep UV using cascaded four-wave mixing processes in a gas. Such cascaded processes exhibit higher efficiencies and broader bandwidths than other schemes for generating ultrashort-pulse light in the deep UV, and will enable many applications in science and technology.

The authors gratefully acknowledge support from the Department of Energy and the National Science Foundation.

*Department of Physics, Colorado School of Mines, Golden, CO.
†Email address: murnane@jila.colorado.edu

[1] C. G. Durfee, S. Backus, M. M. Murnane, and H. C. Kapteyn, Opt. Lett. **22**, 1565 (1997).
[2] A. Rundquist *et al.,* Science **280**, 1412 (1998).
[3] R. Bartels *et al.,* Nature (London) **406**, 164 (2000).
[4] N. A. Anderson *et al.,* Chem. Phys. Lett. **323**, 365 (2000).
[5] A. Rettenberger and R. Haight, Surf. Sci. **414**, 197 (1998).
[6] S. Lejnine *et al.,* Nucleic Acids Res. **27**, 3676 (1999).
[7] T. C. Weinacht, J. Ahn, and P. H. Bucksbaum, Nature (London) **397**, 233 (1999).
[8] V. Blanchet, M. Z. Zgierski, T. Seideman, and A. Stolow, Nature (London) **401**, 52 (1999).
[9] G. C. Bhar, U. Chatterjee, A. M. Rudra, and P. Kumbhakar, Quantum Electron. **29**, 800 (1999).
[10] V. Petrov *et al.,* IEEE J. Sel. Top. Quant. **5**, 1532 (1999).
[11] J. Ringling *et al.,* Opt. Lett. **18**, 2035 (1993).
[12] R. Mahon, T. J. McIlrath, V. P. Myerscough, and D. W. Koopman, IEEE J. Quantum Electron. **15**, 444 (1979).
[13] O. Kittelmann *et al.,* Opt. Lett. **21**, 1159 (1996).
[14] J. H. Glownia, D. R. Gnass, and P. P. Sorokin, J. Opt. Soc. Am. B **11**, 2427 (1994).
[15] A. J. Merriam *et al.,* Phys. Rev. Lett. **84**, 5308 (2000).
[16] C. Dorman, I. Kucukkara, and J. P. Marangos, Phys. Rev. A **61**, 013802 (2000).
[17] G. I. Stegeman, D. J. Hagan, and L. Torner, Opt. Quantum Electron. **28**, 1691 (1996).
[18] X. D. Mu *et al.,* Opt. Lett. **25**, 117 (2000).
[19] V. V. Rostovtseva, A. P. Sukhorukov, V. G. Tunkin, and S. M. Saltiel, Opt. Commun. **22**, 56 (1977).
[20] S. A. Akhmanov, V. A. Martynov, S. M. Saltiel, and V. G. Tunkin, JETP Lett. **22**, 65 (1975).
[21] A. Goehlich, U. Czarnetzki, and H. F. Dobele, Appl. Opt. **37**, 8453 (1998).
[22] H. Crespo, J. T. Mendonca, and A. Dos Santos, Opt. Lett. **25**, 829 (2000).
[23] S. Meyer, B. N. Chichkov, and B. Wellegehausen, J. Opt. Soc. Am. B **16**, 1587 (1999).
[24] S. Backus, C. Durfee, M. M. Murnane, and H. C. Kapteyn, Rev. Sci. Instrum. **69**, 1207 (1998).
[25] P. J. Leonard, At. Data Nucl. Data Tables **14**, 21 (1974).
[26] E. A. J. Marcatili and R. A. Schmeltzer, Bell Syst. Tech. J. **43**, 1783 (1964).
[27] H. J. Lehmaier, W. Leupacher, and A. Penzkofer, Opt. Commun. **56**, 67 (1985).